Comparing and Contrasting the Effects of Iodine Doping on Different Types of Polyacetylene Films

James W. Hall† and Georgia A. Arbuckle*

Department of Chemistry, Rutgers University, Camden, New Jersey 08102

Received August 22, 1994; Revised Manuscript Received October 17, 1995[⊗]

ABSTRACT: A comparison between Shirakawa polyacetylene or S-$(CH)_x$, Naarmann polyacetylene or N-$(CH)_x$, and Tsukamoto polyacetylene or ν-$(CH)_x$ during iodine vapor phase doping has been made. Thin films of each type of polyacetylene were polymerized directly onto quartz crystal substrates. The quartz crystal microbalance (QCM) is used to measure the mass change during doping (oxidation) of polyacetylene with iodine in the vapor phase. For the same mass of dopant, the highest conductivity is observed for ν-$(CH)_x$. The most dense polyacetylene, ν-$(CH)_x$, has the smallest diffusion coefficient on the order of 10^{-14} cm^2/s. The diffusion coefficient for short times (<3000 s) is similar for all three types of polyacetylene (10^{-12} cm^2/s); however, at longer times (10 000−70 000 s), the diffusion coefficients correlate with the densities of the undoped materials.

Introduction

Polyacetylene has attracted much interest since the late 1970s due to the large increase in conductivity observed when the film is exposed to iodine vapor.[1] This simple, conjugated polymer has fascinated chemists, physicists, and material scientists, because it is the first organic polymer to have the electrical and electronic properties of a metal.[2] When Naarmann et al.[3] and subsequently Tsukamoto et al.[4] reported conductivities as high as 10^5 S/cm for stretched polyacetylene films, interest in this air-sensitive conducting polymer was renewed.[5−7] In order to compare these three types of polyacetylene, we have synthesized and characterized both free-standing films and thin films on quartz crystal substrates.[8−10]

We have characterized undoped (nonconducting) free-standing films of S-$(CH)_x$ (traditional Shirakawa polyacetylene[11]), N-$(CH)_x$ (Naarmann et al.[3]), and ν-$(CH)_x$ (Tsukamoto et al.[4]) by ^{13}C CPMAS NMR, FT-IR, resonance Raman spectroscopy (RRS), and scanning electron microscopy (SEM).[9,10] There is a remarkable similarity between the three types. Other studies have also indicated that the electronic properties of N-$(CH)_x$ are similar to those of S-$(CH)_x$.[12] Although our research indicates that catalyst residue remains in N-$(CH)_x$ and ν-$(CH)_x$ even after extensive washing (5−7 days), a higher conductivity is observed after doping for these materials than for S-$(CH)_x$. A more critical factor may be the average conjugation length in each type of polyacetylene. The resonance Raman scattering data indicate that N-$(CH)_x$ and ν-$(CH)_x$ have a longer average conjugation length than S-$(CH)_x$.[10]

One of the principal differences among the free-standing polyacetylene films we studied is their distinct morphologies.[10] The appearance of the films agrees with the reported densities for each type: S-$(CH)_x$ is fibrillar (0.4 g/cm^3),[13] N-$(CH)_x$ is denser with some fibrillar nature (0.85−0.90 g/cm^3),[3] and ν-$(CH)_x$ is the most dense (1.1 g/cm^3).[4] In this paper, we will compare the morphologies of thin films of each type.

In the current study, we report the results of a detailed experimental investigation of the vapor phase iodine doping of thin films of each type of polyacetylene: S-$(CH)_x$, N-$(CH)_x$ and ν-$(CH)_x$. The films were synthesized on quartz crystal substrates according to the methods described in the literature for each type of free-standing polymer. The polymerization times were shortened in order to prepare films on the order of 0.5−4.0 μm thick. The quartz crystal microbalance (QCM) enables small mass changes to be measured during doping.[14] QCM has been used to investigate the polymerization and doping of other conducting polymers such as polypyrrole,[15] polyaniline,[16] and poly(3-methylthiophene).[17] Previously, we have reported on the preliminary results of iodine doping of polyacetylenes.[6−8]

In this study, both the mass change and the resistance have been recorded *in situ* during vapor phase iodine doping. Iodine vapor both oxidizes the polymer (a process referred to as doping, which results in an increase in conductivity) and acts as a counteranion. The increase in mass attributable to the counteranion during doping is measured with the quartz crystal microbalance. The changes in mass and conductivity during doping are compared for each type of polyacetylene. In addition, the changes in mass with time have been used to approximate diffusion coefficients for the iodine doping process.

Experimental Section

Thin films of polyacetylene were polymerized directly onto quartz crystals. The three types of polyacetylene were made with the Ziegler−Natta catalyst based on the methods described in the literature for the synthesis of each type of film: S-$(CH)_x$,[11] N-$(CH)_x$[3], and ν-$(CH)_x$.[4] We have previously described in detail[8] the modified apparatus used to make thin films of each type of polymer on quartz crystal substrates. The thickness of the resulting film can be varied by controlling the amount of catalyst used and the length of time the catalyst is exposed to acetylene gas. Due to the air sensitivity of polyacetylene films, polymerization and subsequent handling of the films were always performed under vacuum or in a purified argon drybox (Vacuum Atmospheres) equipped with a Dri-Train HE-493 continuous-flow argon purification system.

The quartz crystal microbalance (QCM) utilizes 1 in. diameter, 5 MHz AT-cut quartz crystals (McCoy Electronics). The QCM uses a Motorola MC1733 video amplifier based feedback circuit as the oscillator to drive the crystal at its resonant frequency. A Hewlett-Packard 5384A frequency counter was used to monitor the frequency. The data were sent via an IEEE-488 interface bus to a Macintosh SE/30 used to obtain, process, and store data.

†Present Address: Thomas Jefferson University, Philadelphia, PA.

⊗ Abstract published in *Advance ACS Abstracts,* December 1, 1995.

0024-9297/96/2229-0546$12.00/0 © 1996 American Chemical Society

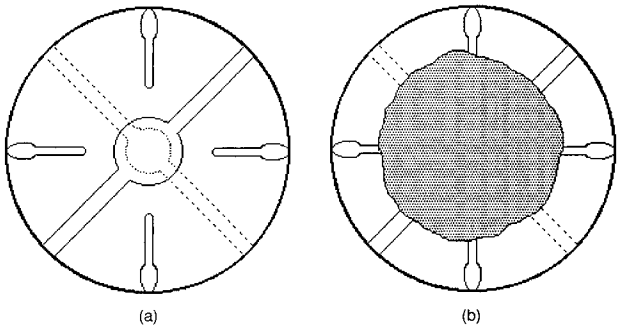

Figure 1. (a) Diagram of quartz crystal electrodes. (b) Region of polymer film.

Gold (2000 Å thick) was evaporated over 200 Å chromium in an asymmetric electrode format.[18] The polyacetylene was synthesized on the larger gold electrode and the film extended to four gold electrode tabs spaced around the circumference of the crystal for conductivity/resistance measurements as shown in Figure 1. We confirmed that the resistance measurements did not interfere with the quartz crystal oscillation. Electrical connections for both frequency and resistance measurements were made to the crystal with flat alligator clips.

In this study, we are using the QCM changes in mass values obtained as a comparison between the three types of polyacetylene rather than as a measure of the absolute mass. The quartz crystal microbalance was calibrated by deposition and stripping of copper in order to correlate the observed frequency changes with mass changes. According to recent reports,[19,20] careful calibration of the QCM is necessary; the theoretical value of 56 Hz cm^{-2} μg^{-1} may not be obtained due to the sensitivity distribution of each individual quartz crystal microbalance. Factors that may influence the calibration value include the thickness of the electrode, the spatial configuration of the electrode, and the properties of the polymer deposited onto the crystal.

Thin polyacetylene films on the quartz crystal were doped by exposure to iodine vapor. The crystal was mounted in the doping apparatus in the drybox. The crystal was held between two PTFE O-rings at room temperature during doping. One side of the crystal faced air; the side on which the film was deposited was under vacuum (<10 μmHg). The doping apparatus contained a bulb of degassed solid iodine. The iodine-containing bulb was held at 0 °C with a constant-temperature bath; the vapor pressure of iodine at 0 °C is 0.0299 mmHg.[21]

The quartz crystal microbalance is routinely used to measure the mass change of materials on the surface of the crystal. The mass change is measured as a frequency change according to the Sauerbrey relationship.[22] After an initial stable frequency reading was recorded, the stopcock to the iodine bulb was opened, exposing the film to iodine vapor. The oscillation frequency decreased (corresponding to a mass increase); the 2-probe resistance was simultaneously recorded. The resistance immediately decreases due to iodine doping of the polyacetylene film. Doping was allowed to continue for varying lengths of time (up to 23 h). Excess iodine absorbed on the surface of the film was removed by immersing the iodine bulb in liquid nitrogen. This caused the frequency to increase by several hundred hertz but had no measurable effect on the resistance readings, indicating that any iodine recovered was not involved in the doping of the polymer. Confirmation that the apparatus had held a vacuum during doping was made by opening the film to a vacuum gauge.

The 4-probe conductivity of each film was measured after doping by the van der Pauw method.[23] Current was passed with a Pine Instrument Co. RDE4 galvanostat or an EG&G PAR 273 potentiostat/galvanostat, and the voltage was monitored with a Keithley 197 DMM. The films were found to be ohmic over the region studied (0.1−10.0 mV).

Scanning electron microscopy was used to measure the thickness of each film. Since the SEM was recorded after doping, no additional carbon coating was needed prior to imaging. A JEOL JSM-6300FV scanning electron microscope at 1−5 keV was used to obtain high resolution images (∼10 000×).

Figure 2. FT-IR of undoped *trans*-polyacetylene: (a) S-$(CH)_x$; (b) N-$(CH)_x$; (c) ν-$(CH)_x$.

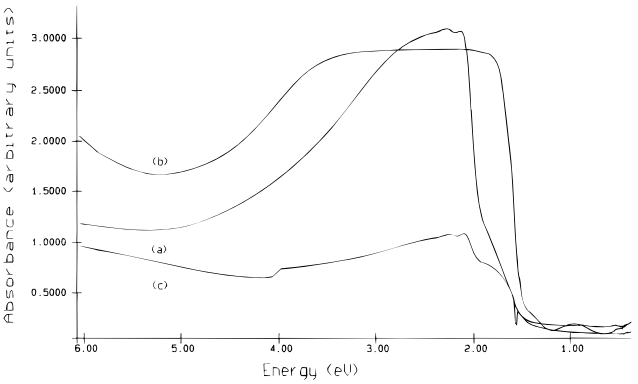

Figure 3. UV−visible−near-infrared spectra of undoped as-made polyacetylene: (a) S-$(CH)_x$; (b) N-$(CH)_x$; (c) ν-$(CH)_x$.

Transmission infrared spectra of thin films of polyacetylene deposited onto NaCl plates were recorded on a Perkin-Elmer 1760-X spectrophotometer under nitrogen purge. Optical absorption spectra of thin films on blank quartz crystals (without gold electrodes) were recorded on a Varian Cary 5 UV−visible−near-infrared spectrophotometer under argon purge.

Results and Discussion

Spectral Characterization and Morphology. The thin films of each type of polyacetylene have been characterized before iodine doping by FT-IR and UV−visible−near-infrared absorption spectroscopy. The FT-IR spectra of isomerized samples of S-$(CH)_x$, N-$(CH)_x$, and ν-$(CH)_x$ are shown in Figure 2. For comparison, the three types of film were simultaneously isomerized by heating in vacuum at 180 °C for 1 h. There is good agreement with the spectra obtained for free-standing films of each type.[10]

The optical spectra of as-made thin films are shown in Figure 3. The structure at the peak in S-$(CH)_x$ and ν-$(CH)_x$ indicates that the samples are primarily in the cis form. The peak also broadens during doping due to doping induced isomerization to the trans form. N-$(CH)_x$ appears to be primarily trans; this is to be expected because the synthesis of N-$(CH)_x$ occurs at room temperature while the other two syntheses are performed at reduced temperatures (−78 °C). The absorption tail at ∼1.4 eV is found for all three types; this is the value commonly taken to approximate the band gap in polyacetylene. Although the band edge seems to be similar, the absorptions at higher eV indicate differences between the three types of polyacetylene. During doping, a low-energy absorption

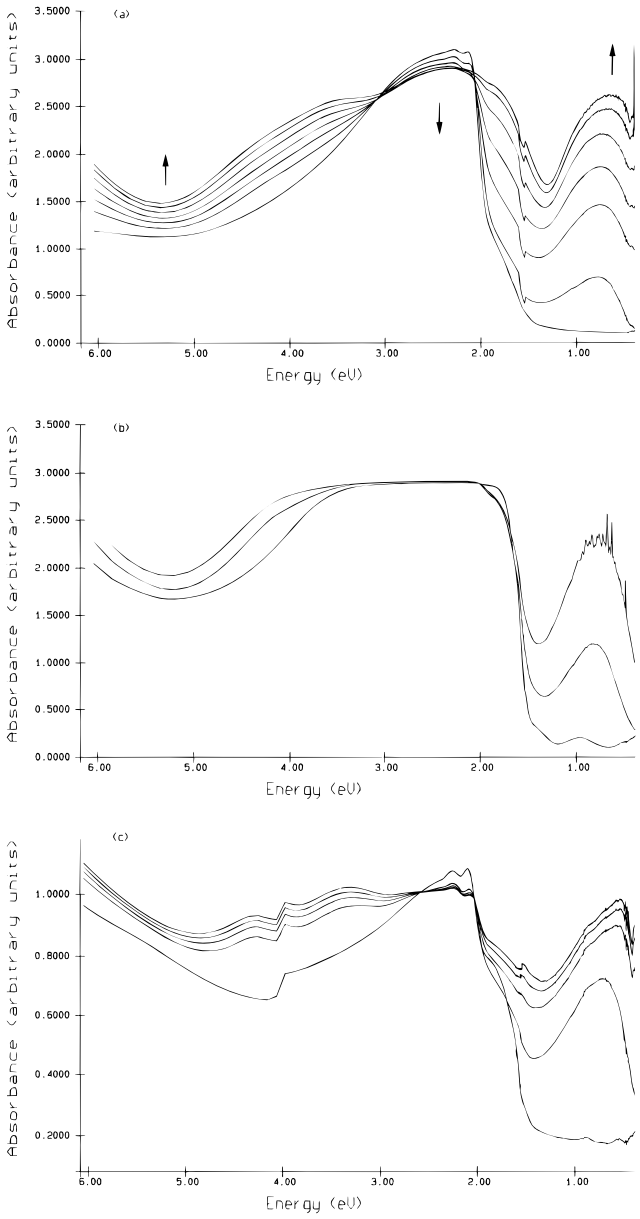

Figure 4. UV−visible−near-infrared spectra during iodine doping of polyacetylene: (a) S-$(CH)_x$; (b) N-$(CH)_x$; (c) ν-$(CH)_x$.

increases at ∼0.7 eV. Spectra taken during iodine vapor phase doping are shown in Figure 4. The detector change occurs at ∼1.6 eV, and the source change is evident in Figure 4c at ∼4 eV. The midgap transition at ∼0.7 eV is somewhat sharper in N-$(CH)_x$ and ν-$(CH)_x$ than in S-$(CH)_x$. Although the three types of polymer are similar, small differences are observed which indicate differences in the band structure of the three types of polymer.

The fibrillar morphology of a S-$(CH)_x$ sample is shown in Figure 5. The SEM shows the cross-sectional view of the polymer deposited on the quartz crystal substrate. The polyacetylene film shown in Figure 5 is approximately 3 μm thick, and this is one of the thicker films prepared. It illustrates well the fibrillar morphology even in the cross-sectional view. The distinct morphology of each type of polyacetylene can also be observed from the scanning electron micrograph images in Figure 6 of the upper side of each type of thin film. For ν-$(CH)_x$, the left side of the image shows the upper side of the film; the right side is the underside. (A small piece of film peeled back so that the underside could be imaged.) The denser nature of ν-$(CH)_x$ is more evident from the

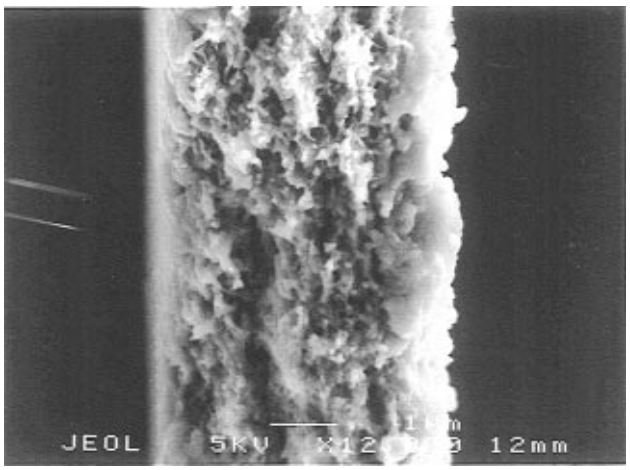

Figure 5. SEM of cross-sectional view of S-$(CH)_x$ (magnification 12 000×).

underside view. The three types of morphology of the thin films agree with the results of free-standing films of each material.[10] The open fibrillar morphology shown in Figure 6a is the spaghetti-like structure most closely associated with conventional S-$(CH)_x$.[24] A more dense morphology has been observed for polyacetylene prepared by a catalyst that has been aged at a temperature above 80 °C[25] as is the case for both N-$(CH)_x$ and ν-$(CH)_x$. Recent studies[25] of the effects of synthesis conditions on the properties of the resulting polyacetylene have indicated that the aging of the catalyst affects the morphology, cis−trans content, stretchability and bulk density of the material. We agree that the denser nature of N-$(CH)_x$ (0.85−0.90 g/cm^3)[3] and ν-$(CH)_x$ (1.1 g/cm^3)[4] compared to S-$(CH)_x$ (0.4 g/cm^3)[13] is important in any attempt to compare the results of the three types of film.

Quartz Crystal Microbalance/Conductivity. *In situ* vapor phase iodine doping of each type of polyacetylene resulted in a frequency decrease (mass increase) and simultaneous resistance decrease (conductivity increase). The QCM measures changes in frequency which are directly proportional to a change in mass according to the Sauerbrey relationship:[22]

$$\Delta f = -[2f_0^2/(\varrho_q \mu_q)^{1/2}]\Delta m/A \qquad (1)$$

where Δf is the measured frequency shift, f_0 the parent frequency of the quartz crystal (5 MHz), Δm the mass change, A the piezoelectrically active area, ρ_q the density of quartz (2.648 g/cm^3), and μ_q the shear modulus (2.947 × 10^{11} dyn/cm^2 for AT-cut quartz).

During iodine doping of the polyacetylene film, the iodine oxidizes the polymer, increasing the conductivity, and also becomes the counteranion to the positive charge created on the polymer film.[2] The frequency changes observed result from the incorporation of the counterion into the film during doping. The dramatic resistance drop (over 8 orders of magnitude) confirms that the film is doped. From the thickness of the film and the resistance change, the conductivity change during iodine doping can be calculated. A typical plot of change in frequency and conductivity vs time is shown in Figure 7 for ν-$(CH)_x$. There is a good correlation between the frequency change observed and the conductivity. Similar plots were obtained for S-$(CH)_x$ and N-$(CH)_x$.

The final conductivities of each type of film calculated using a four-probe measurement[23] are given in Table

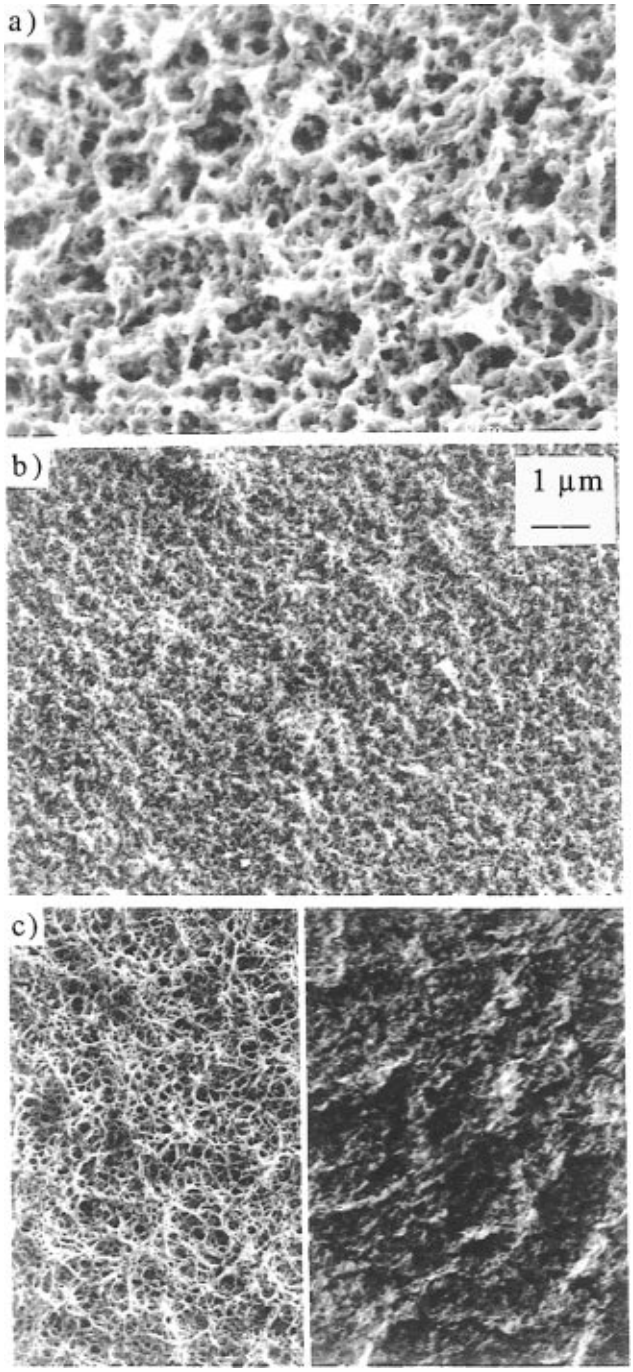

Figure 6. SEM of each type of polyacetylene: (a) S-$(CH)_x$; (b) N-$(CH)_x$; (c) ν-$(CH)_x$ (left, upper side; right, underside) (magnification 10 000×).

Table 1. Type of Film and Conductivity

type of polymer film	conductivity (S/cm)
S-$(CH)_x$	6.4×10^2
N-$(CH)_x$	7.9×10^3
ν-$(CH)_x$	3.2×10^4

1. This is a more exact measure of the conductivity and is usually at least one order of magnitude higher than the two-probe resistance measurements used to calculate the conductivity values in Figures 7−9. It is interesting to note that a significantly higher conductivity was always obtained for ν-$(CH)_x$. More notable is the observation that for the same frequency change (i.e., mass change), a higher conductivity is observed for N-$(CH)_x$ and ν-$(CH)_x$ than for S-$(CH)_x$ during the doping process. A plot of conductivity vs change in frequency is shown in Figure 8 for each type of polyacetylene. This

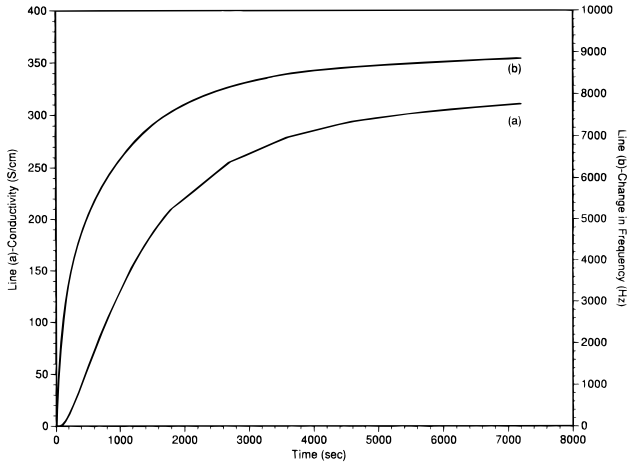

Figure 7. (a) Conductivity (S/cm) and (b) change in frequency (Hz) vs time during iodine doping of ν-$(CH)_x$.

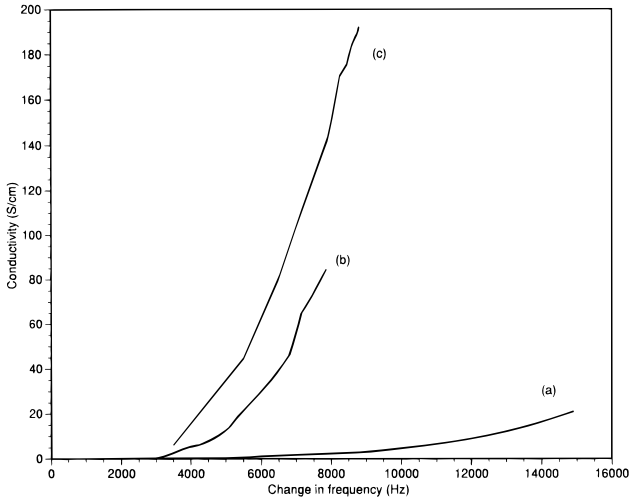

Figure 8. Conductivity (S/cm) vs change in frequency (Hz) of iodine-doped (a) S-$(CH)_x$, (b) N-$(CH)_x$, and (c) ν-$(CH)_x$.

figure shows that the properties of N-$(CH)_x$ and ν-$(CH)_x$ do not simply result in different amounts of dopant uptake, but that the electronic structure causes a higher conductivity for the same change in mass.

Since simply comparing the frequency changes for each type of polyacetylene does not take into account the different densities of the polymers, another type of analysis was made. Using the reported densities for each type of polyacetylene, the measured thickness of each film, and the piezoelectric area of each film, the mole percent iodine in $(CHI_y)_x$ during doping was approximated. A plot of conductivity vs mole percent iodine is shown in Figure 9. As noted from the results in Figure 8, ν-$(CH)_x$ is the most conducting with the smallest percent of iodine. N-$(CH)_x$ is intermediate, with S-$(CH)_x$ having the lowest conductivity even at significantly higher mole percents of iodine. One of the most important results of this study is that the high conductivities shown in Figures 8 and 9 for ν-$(CH)_x$ are for a relatively small amount of iodine dopant.

We have used mole percent iodine because the exact nature of the counterion is known to vary during the doping process. Resonance Raman studies of iodine doping of S-$(CH)_x$ indicate that the counterion may exist as I_3^- or I_5^-.[26,27] This has been confirmed by XPS studies[28,29] and Mössbauer spectroscopy on ^{129}I nuclei.[30,31] Varying ratios of I_5^- to I_3^- have been observed by these techniques. These results indicate that the exact nature of the iodine species in doped polyacetylene

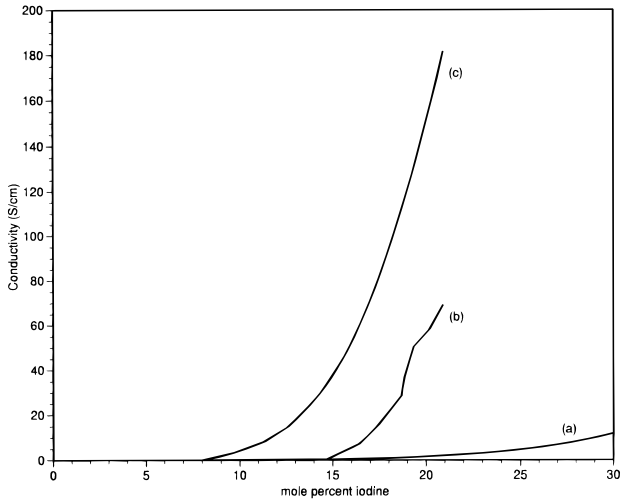

Figure 9. Conductivity (S/cm) vs mole percent iodine in $(CHI_y)_x$: (a) S-$(CH)_x$; (b) N-$(CH)_x$; (c) ν-$(CH)_x$.

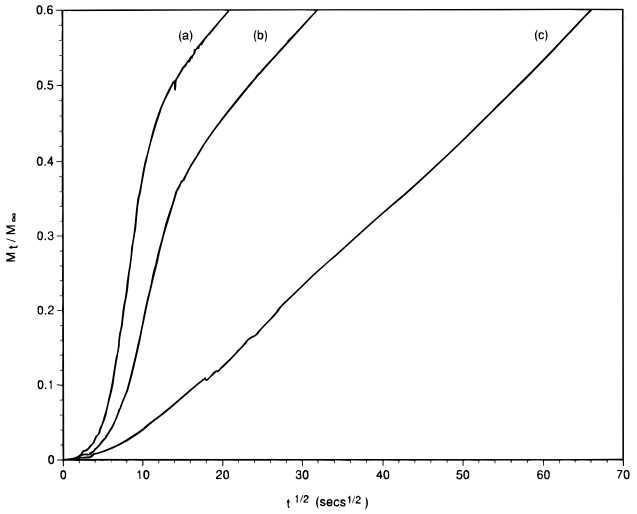

Figure 10. Short-time diffusion plot of difference thicknesses of S-$(CH)_x$: M_t/M_∞ vs $t^{1/2}$ ($s^{1/2}$) [(a)1 μm; (b) 2 μm; (c) 3 μm].

is complex. The equilibrium between I_3^- and I_5^-

$$I_3^- + I_2 \rightleftharpoons I_5^-$$

results in different ratios of I_5^- to I_3^- during the doping process.

The maximum doping level in S-$(CH)_x$ is usually 20−30% I or 8−10% I_3^-.[32] The doping level for N-$(CH)_x$ and ν-$(CH)_x$ shown in Figure 9 is in this range (20%); however, S-$(CH)_x$ appears to have a much higher mass of counterion. If I_5^- is prevalent in S-$(CH)_x$, the actual doping level (i.e., amount of positive charge on the polymer) would be lower for the same change in mass. A possible explanation is that the I_5^- to I_3^- ratio is higher in S-$(CH)_x$ than in N-$(CH)_x$ or ν-$(CH)_x$. This explanation is in agreement with a recent study by Wang et al.[33] which compared S-$(CH)_x$ and ν-$(CH)_x$ (referred to in ref 33 as HCPA (highly conducting polyacetylene)). Polarized resonance Raman studies indicate a larger ratio of I_5^- to I_3^- in S-$(CH)_x$, while in ν-$(CH)_x$ the predominant iodine species is I_3^-. However, their study found that stretching and pumping of the films were related to the I_5^- to I_3^- ratio, while in the present study no mechanical stretching was possible because the thin film was directly deposited onto the quartz substrate. Evacuation of any excess iodine after the conductivity remained constant resulted in no significant change in the iodine doping level in our study.

The open fibrillar morphology of S-$(CH)_x$ (see Figure 6a) may allow the larger I_5^- species to exist, while in N-$(CH)_x$ and ν-$(CH)_x$, the denser morphology may shift the equilibrium toward I_3^-. The ν-$(CH)_x$ (or HCPA) has been reported to have a well-organized X-ray structure with a repeat distance of the iodine chain that implies the primary existence of I_3^- species.[33]

The higher bulk density of films prepared with an aged catalyst has been related to the ability of these films to shrink considerably during the drying process. A thin film fixed on a Teflon substrate would restrict the shrinkage in the thickness direction. This type of in-plane alignment has been reported[25] and appears to be related to the higher conductivities observed when N-$(CH)_x$ and ν-$(CH)_x$ are doped. Alignment may have occurred in our N-$(CH)_x$ and ν-$(CH)_x$ films because of the nature of the synthesis and resulted in the higher conductivities. An analysis of the X-ray crystal structure and the form of counterion in each type of polyacetylene was beyond the scope of the present study, but it deserves further investigation.

Diffusion of Dopant. The diffusion of the iodine into the polymer can be evaluated, since the change in frequency during iodine doping is proportional to the change in mass. The diffusion of gases into polymers has been extensively studied.[34−36] Crank and Park[37] and many others[38−41] use the sorption of vapors in polymers to determine the diffusion coefficient, D. Assuming D is constant and that diffusion is into a plane sheet, the relationship can be expressed as[34]

$$\frac{M_t}{M_\infty} = 1 - \frac{8}{\pi^2}\sum_{m=0}^{m=\infty}\frac{1}{(2m+1)^2}\exp\left[\frac{-D(2m+1)^2\pi^2 t}{l^2}\right] \quad (2)$$

where M_t is the total amount of vapor absorbed at time t, M_∞ is the equilibrium sorption, l is the thickness of the sample, and m is an integer. For long times, eq 2 can be approximated by[34]

$$\frac{M_t}{M_\infty} = 1 - \frac{8}{\pi^2}\exp\left[\frac{-\pi^2 Dt}{l^2}\right] \quad (3)$$

and for short times[34]

$$\frac{M_t}{M_\infty} = \frac{4}{l}\left[\frac{Dt}{\pi}\right]^{1/2} \quad (4)$$

Using eq 4 for short times (<3000 s), a plot of M_t/M_∞ vs $t^{1/2}$ is linear and from the slope, the diffusion coefficient can be determined. Likewise using eq 3 for long times (10 000−70 000 s), a plot of $\ln(1 - M_t/M_\infty)$ vs t is linear and from the slope, the diffusion coefficient can be evaluated.

We have applied these equations to our study. A plot of M_t/M_∞ vs $t^{1/2}$ is shown in Figure 10 for three different thicknesses of S-$(CH)_x$. Similar plots were used to calculate D for N-$(CH)_x$ and ν-$(CH)_x$. A computer-generated slope of each line in Figure 10 results in a diffusion coefficient of $(2-3) \times 10^{-12}$ cm^2/s. The average values are reported in Table 2. The remarkable similarity between the diffusion coefficients for each type of polyacetylene is not unexpected. The values are in agreement with previous studies of vapor phase iodine diffusion in S-$(CH)_x$ ($10^{-14}-10^{-13}$ cm^2/s).[39] Solution phase iodine doping was reported to result in a much higher rate of diffusion ($10^{-7}-10^{-9}$ cm^2/s).[42]

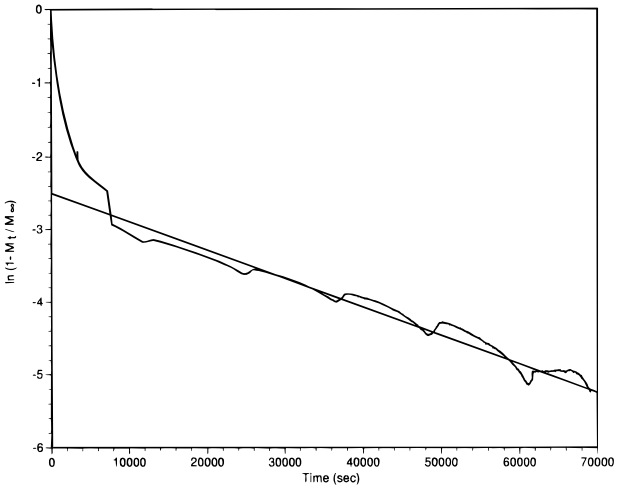

Figure 11. Long-time diffusion plot of ν-$(CH)_x$: $\ln(1 - M_t/M_\infty)$ vs time (s).

Table 2. Diffusion Coefficients

type of polymer film	short time (cm^2/s)	long time (cm^2/s)
S-$(CH)_x$	2×10^{-12}	4×10^{-13}
N-$(CH)_x$	2×10^{-12}	9×10^{-14}
ν-$(CH)_x$	1×10^{-12}	3×10^{-14}

Since all of our studies were performed on thin films, it is not surprising that the diffusion coefficients are similar for short times. However, due to the differences in conductivity, density, and morphology between the three types of polyacetylene, we wanted to also evaluate diffusion over a longer period of time to establish further similarities or differences between them. To apply eq 3 for long times, a plot of $\ln(1 - M_t/M_\infty)$ vs t was made for each type of polyacetylene. The average values are reported in Table 2. A typical plot for ν-$(CH)_x$ is shown in Figure 11. The cyclic anomalies observed occur in all our studies, and we found this to be attributable to a 3 °C temperature variation in the constant-temperature bath over a time period of ~2.5 h. From the linear portion of the plot (10 000−70 000 s) the diffusion coefficient was calculated. Figure 11 also illustrates that for shorter times (<10 000 s), the relationship to t does not hold. Therefore, for shorter times, equation 4 is more appropriate. Although still within a close range, the trend in diffusion coefficients reported in Table 2 correlates with the densities of the undoped polymers; i.e., the densest material results in the smallest diffusion coefficient.

In addition, we have also used eq 5 to evaluate the data of experiments that were stopped before doping was complete.[38]

$$\ln \frac{\partial M}{\partial t} = \ln\left(\frac{8M_\infty D}{l}\right) - \frac{\pi^2 D}{l^2}t \qquad (5)$$

The diffusion coefficients obtained using eq 5 agree with the results for the short times shown in Table 2 and confirm that the diffusion coefficient of 10^{-12} cm^2/s is consistently found for short doping times (<3 000 s).

The diffusion coefficients observed are similar to values found for the diffusion of solid dopants into semiconductors.[39,43] This indicates that the interaction is not simply one of a gas diffusing into a polymer, but rather a chemical reaction (i.e., doping) is also occurring. Initially the diffusion of iodine dopant is into an undoped (nonconducting) polymer. An approximation for the amount of time required for diffusion to occur into a 2 μm thick polymer using the short-time diffusion coefficient (2×10^{-12} cm^2/s) and the diffusion relationship $\langle x \rangle^2 = 2Dt$ is 10 000 s; a thinner film would require less time. This indicates that diffusion of the iodine dopant into the polyacetylene should occur in less than 10 000 s, a time which is consistent with our conductivity studies. As shown in Figure 7, the conductivity change has leveled off within this time. The iodine has diffused into the polymer and the doping of the polyacetylene which results in high conductivities has occurred.

After doping for this period of time, the polymer is conducting. Our studies confirm that iodine continues to diffuse into the polymer. However, the diffusion process is now significantly slower, i.e., reduced by 1−2 orders (10^{-14} cm^2/s). The long-time (>10 000 s) diffusion coefficient is for diffusion into a doped (conducting) polymer. The diffusion at this rate of 10^{-14} cm^2/s into a 1 μm thick polymer will continue for more than 100 000 s. As can be clearly observed in Figure 11, the diffusion process is still steadily continuing after 70 000 s. The diffusion into the doped polymer is slower than into the undoped material and appears to parallel the reported densities of each undoped polymer. This indicates that the long-time diffusion process requires the iodine dopant to move into the interior of the polymer fibrils. We recognize that this is a simplified analysis because the diffusion into the interior of the fibrils would also require charge movement. As the negatively charged iodine diffuses, the positive charge on the polymer chain would also be transferred. In a conjugated polymer, the transport of charge along the polymer would readily occur. Therefore, the limiting process would still be the diffusion of the large iodine anion.

The slower diffusion process does not have a significant effect on the conductivity. The initial diffusion of iodine (<10 000 s) results in doping of the surface of the polymer fibrils with a corresponding conductivity increase. After this doping process is essentially complete, further diffusion into the interior of the polymer fibrils can be measured, but this iodine diffusion does not cause a major conductivity change since the electrical conductivity along the surface of the fibrils would remain constant.

Conclusions

A higher conductivity is found for N-$(CH)_x$ and ν-$(CH)_x$ than for S-$(CH)_x$. Most significantly, for the same mass uptake, N-$(CH)_x$ and ν-$(CH)_x$ exhibit a much higher conductivity. This higher conductivity also corresponds to a lower mole percent doping level than for S-$(CH)_x$. If doping level is calculated using the density of each type of polymer, ν-$(CH)_x$ exhibits a much higher conductivity with a small change in mass, a fact which may have important practical applications. Applications for conducting polymers range from rechargeable batteries to various types of sensors. We believe the electronic structure of ν-$(CH)_x$ to be superior to that of both N-$(CH)_x$ and S-$(CH)_x$ and suggest that further studies be done to corroborate our findings. Our studies agree with the conclusion of Wang et al.[33] that the well-ordered structure of ν-$(CH)_x$ is responsible for the high conductivity.

The diffusion coefficient for the initial stages of iodine vapor phase doping of thin films of these polyacetylenes are on the order of 10^{-12} cm^2/s, which is a reasonable value. Within 10 000 s, a 2 μm thick film has been doped. When diffusion of the iodine is allowed to

continue for considerably longer periods of time, a smaller diffusion coefficient is found, on the order of 10^{-14} cm^2/s. This diffusion is now into a conducting polymer where additional doping throughout the interior of the polymer fibrils has a small effect on conductivity.

Acknowledgment. The authors acknowledge the help of M. A. Alfano, A. L. Kilbert, R.-R. Cheng, D. A. Travis, and D. White in the preparation and study of some samples. Acknowledgment is made to William Romanow for vapor deposition at the Materials Research Facility and to Xue Qin Wang for SEM performed at the LRSM Electron Microscopy Central Facility of the University of Pennsylvania supported by NSF-MRL (Grant DMR91-20668). This work was partially supported by a Bristol-Myers Squibb Company Award of Research Corporation and the National Science Foundation (REU Supplement to Grant DMR91-11356). G.A.A. acknowledges a NSF Young Investigator Award (Grant DMR92-58167) and wishes to thank the reviewers for helpful comments.

References and Notes

(1) (a) Chiang, C. K.; Fincher, C. R.; Park, Y. W.; Heeger, A. J.; Shirakawa, H.; Louis, E. J.; Gau, S. C.; MacDiarmid, A. G. *Phys. Rev. Lett.* **1977,** *39*, 1098. (b) Chiang, C. K.; Druy, M. A.; Gau, S. C.; Heeger, A. J.; Louis, E. J.; MacDiarmid, A. G.; Park, Y. W.; Shirakawa, H. *J. Am. Chem. Soc.* **1978**, *100*, 1013. (c) Chiang, C. K.; Park, Y. W.; Heeger, A. J.; Shirakawa, H.; Louis, E. J.; MacDiarmid, A. G. *J. Chem. Phys.* **1978**, *69*, 5098.

(2) (a) Chien, J. C. W. *Polyacetylene: Chemistry, Physics and Material Science*; Academic Press: Orlando, 1984. (b) Skotheim, T. A. Ed. *Handbook of Conducting Polymers*; Marcel Dekker: New York, 1986. (c) Krivoshei, I. V.; Skorobogatov, V. M. *Polyacetylene and Polyarylenes: Synthesis and Conductive Properties*; Gordon and Breach Science Publishers: Amsterdam, 1991.

(3) (a) Naarmann, H.; Theophilou, N. *Synth. Met.* **1987**, *22*, 1. (b) Theophilou, N.; Naarmann, H. In *Conducting Polymers*; Alcacer, L., Ed.; D. Reidel Publishing Co.: Dordrecht, 1987. (c) Schimmel, Th.; Reiss, W.; Gmeiner, J.; Schwoerer, M.; Naarmann, H.; Theophilou, N. *Solid State Commun.* **1988**, *65*, 1311. (d) Basecu, N.; Liu, Z.-X.; Moses, D.; Heeger, A. J.; Naarmann, H.; Theophilou, N. *Nature* **1987**, *327*, 403.

(4) (a) Tsukamoto, J.; Takahashi, A.; Kawasaki, K. *Jpn. J. Appl. Phys.* **1990**, *29*, 125. (b) Tsukamoto, J.; Takahashi, A. *Synth. Met.* **1991**, *41*, 7.

(5) MacDiarmid, A. G.; Epstein, A. J. in *Conjugated Polymeric Materials: Opportunities in Electronics, Optoelectronics, and Molecular Electronics*; Bredas, J. L., Chance, R. R., Eds.; Kluwer Academic Publishers: Dordrecht, The Netherlands, 1990; p 53.

(6) Arbuckle, G. A.; Buecheler, N. M.; Clark, C. G.; Pepe, S.; Wille, A. E. *Proceedings of the American Chemical Society Division of Polymeric Materials: Science and Engineering*, American Chemical Society: Washington, DC, 1991; Vol. 64, p 269.

(7) (a) Hall, J. W.; Arbuckle, G. A. 32nd Annual Eastern Analytical Symposium, Somerset, NJ, November 1993. (b) Alfano, M. A.; Cheng, R.-R.; Kilbert, A. L.; White, D.; Arbuckle, G. A. *Abstracts of Papers*, 27th Middle Atlantic Regional Meeting of the American Chemical Society, Hempstead, NY, June 1993; paper 295. (c) Buecheler, N. M.; Arbuckle, G. A. *Abstracts of Papers*, 25th Middle Atlantic Regional Meeting of the American Chemical Society, Newark, DE, May 1991; paper 229.

(8) Arbuckle, G. A.; Buecheler, N. M.; Clark, C.; Wille, A. *Synth. Met.* **1994**, *63*, 35.

(9) Arbuckle, G. A.; Buecheler, N. M.; Valentine, K. G. *Chem. Mater.* **1994**, *6*, 569.

(10) Arbuckle, G. A.; Buecheler, N. M.; Hall, J. W.; Valentine, K. G.; Lefrant, S.; Mevellec, J. Y.; Mulazzi, E., submitted to *Phys. Rev. B*.

(11) (a) Shirakawa, H.; Ikeda, S. *Polym. J.* **1971,** *2*, 231. (b) Ito, T.; Shirakawa, H.; Ikeda, S. *J. Polym. Sci., Polym. Chem. Ed.* **1974**, *12*, 11.

(12) (a) Theophilou, N.; Swanson, D. B.; MacDiarmid, A. G.; Chakraborty, A.; Javadi, H. H. S.; McCall, R. P.; Treat, S. P.; Zuo, F. Epstein, A. J. *Synth. Met.* **1989**, *28*, D35. (b) Javadi, H. H. S.; Chakroborty, A.; Li, C.; Theophilou, N.; Swanson, D. B.; MacDiarmid, A. G.; Epstein, A. J. *Phys. Rev. B* **1991**, *43*, 2183.

(13) Karasz, F. E.; Chien, J. C. W.; Galkiewicz, R.; Wnek, G.; Heeger, A. J.; MacDiarmid, A. G. *Nature* **1979,** *282*, 286.

(14) Lu, E.; Czanderna, A. W., Eds. *Applications of Piezoelectric Quartz Crystal Microbalances. Methods and Phenomena*; Elsevier: New York, 1984; Vol. 7.

(15) Baker, C.; Reynolds, J. *J. Electroanal. Chem.* **1988**, *251*, 307.

(16) Orata, D.; Buttry, D. A. *J. Am. Chem. Soc.* **1987**, *109*, 3574.

(17) Servagent, S.; Vieil, E. *J. Electroanal. Chem.* **1990**, *280*, 227.

(18) Ward, M. D. *J. Phys. Chem.* **1988,** *92*, 2049.

(19) (a) Hillier, A. C.; Ward, M. D. *Anal. Chem.* **1992**, *64*, 2539. (b) Buttry, D. A.; Ward, M. D. *Chem. Rev.* **1992**, *92*, 1355. (c) Ward, M. D.; Buttry, D. A. *Science* **1990**, *249*, 1000.

(20) Cumpson, P. J.; Seah, M. P. *Meas. Sci. Technol.* **1990**, *1*, 544.

(21) *International Critical Tables*. National Academy of Science, Maple Press Co.: York, PA, 1928; Vol. III, p 201.

(22) Sauerbrey, G. *Z. Phys.* **1959**, *155*, 206.

(23) van der Pauw, L. J. *Philips Res. Rep.* **1958**, *13*, 1.

(24) Epstein, A. J.; Rommelmann, H.; Fernquist, R.; Gibson, H. W.; Druy, M. A.; Woerner, T. *Polymer* **1982**, *23*, 1211.

(25) Shirakawa, H.; Zhang, Y.-X.; Okuda, T.; Sakamaki, K.; Akagi, K. *Synth. Met.* **1994**, *65*, 93.

(26) (a) Shirakawa, H.; Sasaki, T.; Ikeda, S. *Chem. Lett.* **1978**, 1113. (b) Harada, I.; Tasumi, M.; Shirakawa, H.; Ikeda, S. *Chem. Lett.* **1978**, 1411.

(27) Lefrant, S.; Lichtmann, L. S.; Temkin, H.; Fitchen, D. B.; Miller, D. C.; Whitwell, G. E.; Burlitch, J. M. *Solid State Commun.* **1979**, *29*, 191.

(28) Ikemoto, I.; Sakairi, M.; Tsutsumi, T.; Kuroda, H.; Harada, I.; Tasumi, M.; Shirakawa, H.; Ikeda, S. *Chem. Lett.* **1979**, 1189.

(29) Salaneck, W. R.; Thomas, H. R.; Bigelow, R. W.; Duke, C. B.; Plummer, E. W.; Heeger, A. J.; MacDiarmid, A. G. *J. Chem. Phys.* **1980**, *72*, 3674.

(30) Kaindl, G.; Wortmann, G.; Roth, S.; Menke, K. *Solid State Commun.* **1982**, *41*, 75.

(31) (a) Matsuyama, T.; Sakai, H.; Yamaoka, H.; Maeda, Y.; Shirakawa, H. *Solid State Commun.* **1981**, *40*, 563. (b) Matsuyama, T.; Sakai, H.; Yamaoka, H.; Maeda, Y.; Shirakawa, H. *J. Phys. Soc. Jpn.* **1983**, *52*, 2238.

(32) Baughmann, R. H.; Hsu, S. L.; Pez, G. P.; Signorelli, A. J. *J. Chem. Phys.* **1978**, *68*, 5405.

(33) Wang, D.; Tsukamoto, J.; Takahashi, A.; Muraki, N.; Katagiri, G. *Synth. Met.* **1994**, *65*, 117.

(34) Vieth, W. R. *Diffusion In and Through Polymers: Principles and Applications*; Hanser Publishers: Munich, 1991.

(35) Crank, J.; Park, G. S., Eds. *Diffusion in Polymers*; Academic Press: New York, 1968.

(36) Crank, J. *The Mathematics of Diffusion*; Clarendon Press: Oxford, 1975.

(37) Crank, J.; Park, G. S. In *Diffusion in Polymers*; Crank, J., Park, G. S., Eds.; Academic Press: New York, 1968; Chapter 1.

(38) Chalykh, A. E. in *Experimental Methods of Polymer Physics: Measurement of Mechanical Properties, Viscosity and Diffusion*; Malkin, A. Ya., Ed.; Mir Publishers: Moscow, 1979 (English translation by G. Leib, Prentice-Hall: Englewood Cliffs: NJ, 1983; Part 5).

(39) Kiess, H.; Meyer, W.; Baeriswyl, D.; Harbeke, G. *J. Electron. Mater.*, **1980**, *9*, 763.

(40) (a) Benoit, C.; Rolland, M.; Aldissi, M.; Rossi, A.; Cadene, M.; Bernier, P. *Phys. Status Solidi A* **1981**, *68*, 209. (b) Rolland, M.; Aldissi, M.; Cadene, M.; Bresse, J. F.; Benoit, C. *Rev. Phys. Appl.* **1982**, *17*, 373.

(41) Danno, T.; Miyasaka, K.; Ishikawa, K. *J. Polym. Sci., Polym. Phys. Ed.* **1983**, *21*, 1527.

(42) (a) Beniere, F.; Haridoss, S.; Louboutin, J. P.; Aldissi, M.; Fabre, J. M. *J. Phys. Chem. Solids* **1981**, *42*, 649. (b) Louboutin, J. P.; Beniere, F. *J. Phys. Chem. Solids* **1982**, *43*, 233.

(43) Jost, W. In *Diffusion in Solids, Liquids and Gases*; Hutchinson, E., Ed.; Academic Press: New York, 1952.

MA946424T